Science
AAAS

A "Silent" Polymorphism in the *MDR*1 Gene Changes Substrate Specificity

Chava Kimchi-Sarfaty *et al.*

Science **315**, 525 (2007);
DOI: 10.1126/science.1135308

dient with decay length $\lambda = 20.2$ μm, whereas, in these in vivo conditions, Wg made a short-range gradient with $\lambda = 5.8 \pm 2.04$ μm (Figs. 3I and 4A). Which kinetic parameter could account for this difference? Because Dpp and Wg have inherently different properties—Wg is a lipid-modified molecule (*20*); Dpp is not (*21*)—they are likely to display different mechanisms and kinetics of spreading through the epithelium.

The shorter decay length of the Wingless gradient was due to a higher degradation rate of GFP-Wingless, by a factor of 5, and to a lesser extent its smaller diffusion coefficient (Fig. 4). Although the Gal4 driver was the same in the Dpp and Wg experiments, the production rate of Wg was about seven times that of Dpp, which implied that their maturation and secretion were controlled differently. In addition, while 62% of the Dpp molecules were immobile, the Wg pool was almost fully mobile at 25°C ($\psi = 9.2 \pm 13\%$), although, unlike Dpp, a significant immobile fraction appeared at higher experimental temperatures (Fig. 3, K and N). The different immobile fractions of Dpp and Wg at 25°C validated the specificity of the Dpp immobile fraction. Thus, the immobile fraction was not an artifact of incomplete recovery in sick cells. Finally, in contrast to Dpp, Wg transport and degradation were independent of Dynamin endocytosis (Fig. 3, K to O). Indeed, Wg movement has been suggested to be Dynamin-independent (*6*, *22*). In addition, expression of dominant-negative Dynamin and/or long-term thermosensitive *shibire* block caused an extension of the gradient in the wing (*5*, *22*, *23*), which was attributed to decreased degradation (*5*, *22*). Our FRAP approach studying the results of an acute block suggests that endocytosis is not required for Wg transport and degradation or, alternatively, that endocytosis of Wg is Dynamin-independent.

Altogether, the GFP-Wingless FRAP experiments (i) validated our FRAP assay and shibire-rescue experiment; (ii) indicated that different morphogen gradients can be generated by independently fine-tuning D, k, ν, and ψ; and (iii) showed that different morphogens may use different mechanisms of transport and cellular machineries (e.g., Dynamin-dependent versus Dynamin-independent transport) to achieve the formation of morphogen gradients.

References and Notes

1. T. Y. Belenkaya *et al.*, *Cell* **119**, 231 (2004).
2. E. V. Entchev, A. Schwabedissen, M. González-Gaitán, *Cell* **103**, 981 (2000).
3. K. Kruse, P. Pantazis, T. Bollenbach, F. Jülicher, M. González-Gaitán, *Development* **131**, 4843 (2004).
4. A. D. Lander, Q. Nie, F. Y. Wan, *Dev. Cell* **2**, 785 (2002).
5. E. Piddini, F. Marshall, L. Dubois, E. Hirst, J.-P. Vincent, *Development* **132**, 5479 (2005).
6. M. Strigini, S. M. Cohen, *Curr. Biol.* **10**, 293 (2000).
7. A. A. Teleman, S. M. Cohen, *Cell* **103**, 971 (2000).
8. K. Basler, G. Struhl, *Trends Genet.* **10**, 187 (1994).
9. J. Lippincott-Schwartz, N. Altan-Bonnet, G. H. Patterson, *Nat. Cell Biol.* **5** (suppl.), S7 (2003).
10. G. Carrero, D. McDonald, E. Crawford, G. de Vries, M. J. Hendzel, *Methods* **29**, 14 (2003).
11. A. Charpilienne *et al.*, *J. Biol. Chem.* **276**, 29361 (2001).
12. D. Axelrod, D. E. Koppel, J. Schlessinger, E. Elson, W. W. Webb, *Biophys. J.* **16**, 1055 (1976).
13. J. Ellenberg, J. Lippincott-Schwartz, *Methods* **19**, 362 (1999).
14. R. Swaminathan, C. P. Hoang, A. S. Verkman, *Biophys. J.* **72**, 1900 (1997).
15. G.-H. Baeg, E. M. Selva, R. M. Goodman, R. Dasgupta, N. Perrimon, *Dev. Biol.* **276**, 89 (2004).
16. C. Han, D. Yan, T. Y. Belenkaya, X. Lin, *Development* **132**, 667 (2005).
17. T. Lecuit, S. M. Cohen, *Development* **125**, 4901 (1998).
18. J. Klingauf, E. T. Kavalali, R. W. Tsien, *Nature* **394**, 581 (1998).
19. S. Pfeiffer, S. Ricardo, J.-B. Manneville, C. Alexandre, J.-P. Vincent, *Curr. Biol.* **12**, 957 (2002).
20. K. Willert *et al.*, *Nature* **423**, 448 (2003).
21. J. Groppe *et al.*, *J. Biol. Chem.* **273**, 29052 (1998).
22. E. S. Seto, H. J. Bellen, *J. Cell Biol.* **173**, 95 (2006).
23. A. F. Rives, K. M. Rochlin, M. Wehrli, S. L. Schwartz, S. DiNardo, *Dev. Biol.* **293**, 268 (2006).

24. We thank J.-P. Vincent and A. Charpilienne for reagents, C. P. Heisenberg and E. Entchev for critical reading of the manuscript, as well as all members of the M.G.-G. and F.J. groups. This work was supported by the Max Planck Society, Deutsche Forchungsgemeinschaft, Volkswagen Stiftung, the European Union, and the Human Frontier Science Program.

Supporting Online Material

www.sciencemag.org/cgi/content/full/315/5811/521/DC1
Materials and Methods
SOM Text
Figs. S1 to S8
Table S1
Movies S1 to S3

2 October 2006; accepted 6 December 2006
10.1126/science.1135774

A "Silent" Polymorphism in the *MDR*1 Gene Changes Substrate Specificity

Chava Kimchi-Sarfaty,*† Jung Mi Oh,†‡ In-Wha Kim, Zuben E. Sauna, Anna Maria Calcagno, Suresh V. Ambudkar, Michael M. Gottesman†

Synonymous single-nucleotide polymorphisms (SNPs) do not produce altered coding sequences, and therefore they are not expected to change the function of the protein in which they occur. We report that a synonymous SNP in the *Multidrug Resistance* 1 (*MDR*1) gene, part of a haplotype previously linked to altered function of the *MDR*1 gene product P-glycoprotein (P-gp), nonetheless results in P-gp with altered drug and inhibitor interactions. Similar mRNA and protein levels, but altered conformations, were found for wild-type and polymorphic P-gp. We hypothesize that the presence of a rare codon, marked by the synonymous polymorphism, affects the timing of cotranslational folding and insertion of P-gp into the membrane, thereby altering the structure of substrate and inhibitor interaction sites.

The *MDR*1 gene product, the adenosine triphosphate (ATP)–binding cassette (ABC) transporter ABCB1 or P-gp, is an ATP-driven efflux pump contributing to the pharmacokinetics of drugs that are P-gp substrates and to the multidrug resistance of cancer cells (*1*, *2*). To date, more than 50 single-nucleotide polymorphisms (SNPs) have been reported for *MDR*1 (www.ncbi.nlm.nih.gov/SNP/GeneGt.cgi?geneID=5243). One of these, a synonymous SNP in exon 26 (C3435T), was sometimes found to be associated with altered P-gp activity (*3*–*6*) and, when it appears in a haplotype, with reduced functionality (*7*). This association may be explained in different ways. Perhaps it is because C3435T is in linkage disequilibrium with other common functional nonsynonymous polymorphisms such as G2677T. In fact, the C1236T (a synonymous SNP), G2677T, and C3435T polymorphisms are part of a common haplotype (*8*, *9*). Another possible explanation is that allele-specific differences in mRNA folding could influence splicing, processing, or translational control and regulation (*10*, *11*). A third possibility is that the effect of the C3435T polymorphism on the levels of cell surface P-gp activity or its function is rather modest or drug-specific. Finally, numerous environmental factors are known to affect the expression and phenotypic activity of P-gp (*12*).

To determine whether the C3435T polymorphism actually does affect P-gp activity, we expressed wild-type and polymorphic P-gps in HeLa cells with the use of a transient expression system (*13*). The same experiments were carried out on BSC-1 (epithelial cells of African green monkey kidney origin), Vero-76 (monkey kidney cells), and 12E1 (CEM human cells) cell lines (*14*), with similar results, indicating that this phenomenon is not specific to HeLa cells.

Laboratory of Cell Biology, Center for Cancer Research, National Cancer Institute, Bethesda, MD 20892, USA.

*Present address: Center for Biologics Evaluation and Research, Food and Drug Administration, 29 Lincoln Drive, Room 316, Bethesda, MD 20892, USA.

†To whom correspondence should be addressed. E-mail: mgottesman@nih.gov (M.M.G.); jmoh@snu.ac.kr (J.M.O.); kimchi@cber.fda.gov (C.K.-S.)

‡Present address: College of Pharmacy, Seoul National University, Seoul 151-742, South Korea.

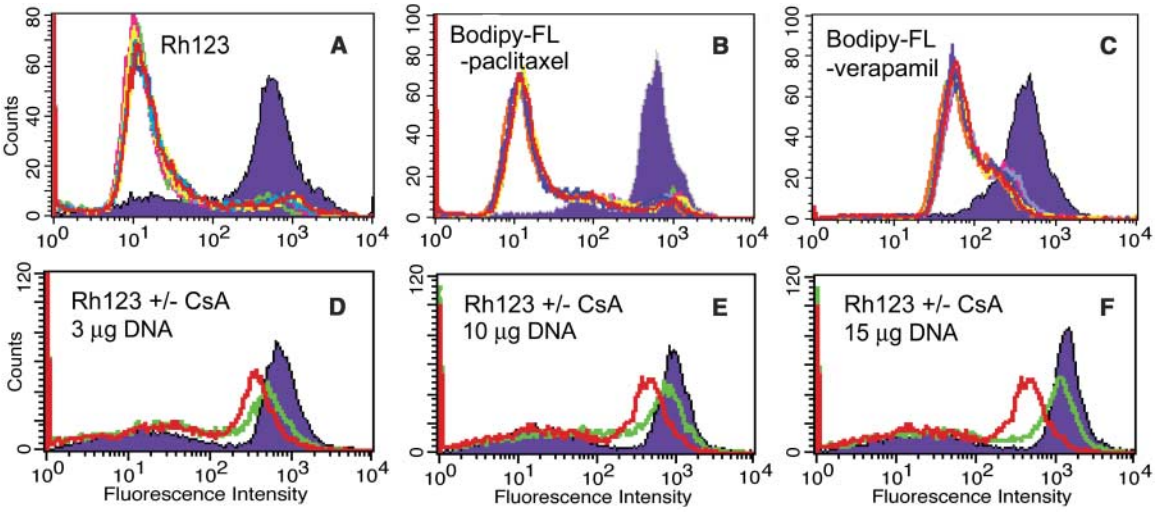

Fig. 1. Drug transport function of wild-type MDR1 and seven MDR1 SNPs and haplotypes. The drug efflux from vaccinia virus infected/transfected HeLa cells was determined by FACS analysis. Cells were transfected with pTM1 (control; purple), pTM1-*MDR*1 (wild-type P-gp; green), C1236T (pink), G2677T (lavender), C3435T (orange), C1236T-G2677T (blue), C1236T-C3435T (yellow), G2677T-C3435T (light blue), and C1236T-G2677T-C3435T (red). (**A**) 0.5 μM Rh123; (**B**) 0.1 μM bodipy-FL-paclitaxel; (**C**) 0.5 μM bodipy-FL-verapamil. (**D** to **F**) Effect of plasmid DNA concentration during infection/transfection on Rh123 efflux (0.5 μM) in the presence of an inhibitor, 10 μM CsA; infected/transfected DNA, (D) 3 μg, (E) 10 μg, (F) 15 μg.

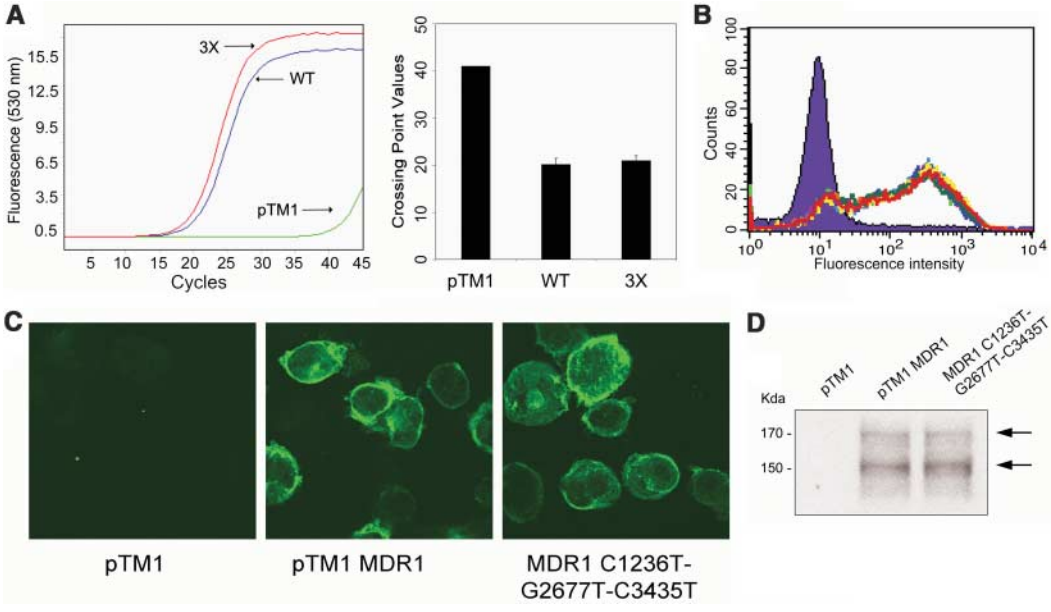

Fig. 2. mRNA levels and P-gp expression in the vaccinia expression system. (**A**) Analysis of pTM1 only, wild-type *MDR*1, and the haplotype C1236T-G2677T-C3435T (3X) with real-time quantitative RT-PCR. Crossing-point values for the graph on the left are plotted in the histogram. (**B**) Assessment of cell surface expression, using MRK16 mAb of all nine constructs as described in Fig. 1. (**C**) Confocal assessment of MDR1 expression, using MRK16 mAb with fluorescein isothiocyanate–conjugated secondary antibody of pTM1 (control; left panel), pTM1-MDR1 (wild-type P-gp; middle panel), and C1236T-G2677T-C3435T (right panel). (**D**) Immunoblot analysis of pTM1 only, wild-type MDR1, and the haplotype C1236T-G2677T-C3435T (2 μg protein/lane) with C219 mAb (*14*). The mature fully glycosylated (~170 kD) and immature P-gp bands (~150 kD) are marked by arrows (*19*).

Assays for P-gp's transport function with the fluorescent substrates Rhodamine 123 (Rh123), bodipy-FL-paclitaxel, bodipy-FL-verapamil, daunorubicin, bodipy-FL-vinblastine, and calcein-AM (*14*, *15*) were performed on HeLa cells expressing the MDR1 wild-type; polymorphisms at C1236T, G2677T, or C3435T; and haplotypes consisting of these polymorphic variant combinations: C1236T-G2677T, C1236T-C3435T, G2677T-C3435T, and C1236T-G2677T-C3435T. The functions of P-gp for all single-polymorphism plasmids as well as for wild-type MDR1, as measured by intracellular accumulation or by efflux of fluorescent compounds, were not distinguishable under standard conditions (*14*). HeLa cells expressing double- and triple-haplotype mutants also revealed results similar to those for the single mutants (Fig. 1, A to C). However, the P-gp inhibitors cyclosporin A (CsA) and verapamil (fig. S1) were less effective against all the substrates in cells expressing the double or triple haplotypes carrying C3435T relative to the wild type, the SNPs, or the haplotype that does not carry C3435T. Thus, it is not the presence of the nonsynonymous polymorphism G2677T that results in the phenotype, but rather the presence of C3435T in combination with one or two of the other polymorphisms.

We next tested to see whether these differences correlated with the concentrations of transduced plasmid DNA. The expression and function of all transduced cells were measured by fluorescence-activated cell sorting (FACS) with MRK16 monoclonal antibody (mAb) staining and by Rh123 in the presence of CsA, respectively (*14*). The differences in inhibition by CsA and Rh123 between the cells expressing wild-type MDR1 and the haplotype C1236T-G2677T-C3435T were more distinct as the concentration of the DNA increased (Fig. 1, D to F). These data suggest that the differences were more pronounced at higher levels of mRNA where more P-gp was being translated in the cells. The expression levels of P-gp from the vaccinia infection/transfection system and cells of normal human adrenal glands were found to be comparable (fig. S2).

Figure S1, C to E, shows that the haplotypes including C3435T had altered susceptibility to verapamil, but not to rapamycin (fig. S1F) (*14*). When the cells were incubated with the inhibitors before adding the fluorescent substrates, as opposed to simultaneous incubation with the drugs, the same pattern was observed. Bodipy-FL-verapamil, wild-type P-gp, and the haplotype (C1236T-G2677T-C3435T) exhibited different

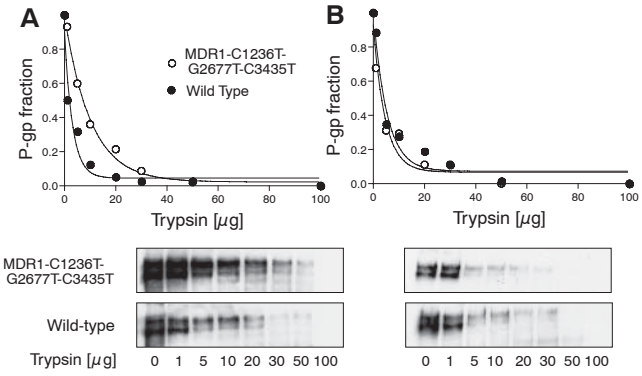

Fig. 3. Determining the sensitivity of wild-type and the haplotype C1236T-G2677T-C3435T P-gp to trypsin. Crude membranes prepared from vTF7-3 infected/transfected HeLa cells expressing wild-type MDR1 or the haplotype C1236T-G2677T-C3435T were treated with increasing concentrations of trypsin and the disappearance of the P-gp band was quantified as described above. (**A**) Experiment performed in the absence of verapamil; IC_{50} = 2.1 μg (wild type), 7.1 μg (C1236T-G2677T-C3435T). The mature (170 kD) and immature (150 kD) P-gp bands were also analyzed separately; IC_{50} = 0.68 μg (wild-type immature), 2.9 μg (haplotype immature), 2.8 μg (wild-type mature), 10.8 μg (haplotype mature). (**B**) Same experiment in the presence of 30 μM verapamil; IC_{50} = 3.7 μg (wild type), 3.3 μg (C1236T-G2677T-C3435T). Values for the mature and immature P-gp bands: IC_{50} = 2.5 μg (wild-type immature), 2.5 μg (haplotype immature), 3.6 μg (wild-type mature), 3.2 μg (haplotype mature). Immunoblots with C219 mAb are shown at the bottom.

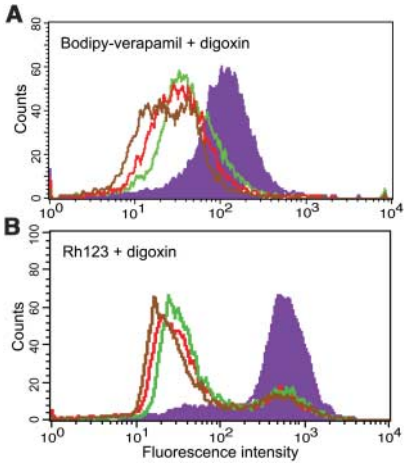

Fig. 4. Drug transport function of wild-type and two MDR1 haplotypes. The drug efflux of vaccinia infected/transfected HeLa cells was determined by FACS analysis (*14*). Cells were transfected with pTM1 (control; purple), MDR1, (wild-type P-gp; green), C1236T-G2677T-C3435T (red), and C1236T-G2677T-C3435A (brown). (**A**) 0.5 μM bodipy-FL-verapamil in the presence of 500 μM digoxin; (**B**) 0.5 μM Rh123 in the presence of 150 μM digoxin.

accumulations in a concentration-dependent manner, suggesting a change in affinity (fig. S3).

Synonymous SNPs or mutations can cause inactivation of the native splicing donor site, which results in a premature stop codon (*16*) or exon skipping, yielding a shorter mRNA. A previous report indicated that the polymorphism C3435T resulted in decreased levels of mRNA expression (*17*). We therefore compared mRNA levels (*14*) in the wild-type and haplotype (C1236T-G2677T-C3435T) with the use of real-time quantitative reverse transcription polymerase chain reaction (RT-PCR), which revealed equivalent mRNA levels (Fig. 2A). Western blots using C219 mAb showed comparable total cell expression of P-gp, and the infected/transfected cells expressed the same levels of P-gp as determined by FACS assays and immunohistochemical staining with MRK16 mAb (Fig. 2, B and C). This result was reproduced in different cell lines including BSC-1, Vero-76, and 12E1 (fig. S4). The complete amino acid sequence of MDR1 haplotype C1236T-G2677T-C3435T protein was identical to the predicted sequence.

We hypothesized that a conformation difference between wild-type and haplotype P-gp might explain these results. Indeed, UIC2 (*14*), a conformation-sensitive mAb, alone or in combination with CsA or vinblastine at 37°C, revealed pronounced differences in binding consistent with altered conformations in the haplotype (fig. S5) (*18*). To determine whether there are subtle differences in the folding of wild-type and haplotype P-gp, we compared their relative susceptibility to trypsin. Figure 3 shows the disappearance of the P-gp band as a function of trypsin concentration. The concentration required for 50% degradation (IC_{50}, here expressed as μg trypsin) was greater for haplotype P-gp than for wild-type P-gp by a factor of about 3.4; this result implies that the two have slightly different tertiary structures. Both wild-type and haplotype P-gps had comparable IC_{50} (μg trypsin) values in the presence of verapamil, which suggests that the altered conformation can be corrected by drug interaction with P-gp. The immature, core-glycosylated form of P-gp (150-kD band) was more sensitive to trypsin than the mature, glycosylated form, consistent with (*19*), by a factor of 5. However, the ratios (wild-type:haplotype) of the IC_{50} (μg trypsin) values were comparable for the mature and immature bands (3.86 μg versus 4.4 μg). Thus, it is unlikely that altered glycosylation is responsible for the functional differences observed.

The use of rare codons appears to influence the translation rate, which in turn affects protein folding (*20*–*25*), with the third base in the codon having the largest effect (*26*). We hypothesize that as the cell produces more P-gp (Fig. 1, D to F), the role of codon usage may become more critical when certain tRNA species become depleted. The codon usage for the SNP at position 12/1236 with GGC changed to GGT (both encode Gly) changes from 34% [relative synonymous codon usage (RSCU), 22.4] to 16% (RSCU, 10.8). The SNP at position 21/2677 that changes GCT (Ala) to TCT (Ser) also uses a less common codon (26% to 18%; RSCU values change from 18.5 to 15.1). The SNP at position 26/3435 that changes the codon from ATC (Ile) to ATT (Ile) reduces the codon usage from 47% to 35% (RSCU values change from 20.9 to 15.8). Clusters of rare codon usage (table S1) occur both upstream and downstream of each of these SNPs. Codon usage rates are similar in humans and monkeys, which explains the similarity in the results with all transduced cells (*27*).

To test whether codon usage compromises P-gp function, we introduced C3435A (isoleucine codon usage for ATA is 18%, RSCU 7.4) to produce the haplotype C1236T-G2677T-C3435A. Functional assays using bodipy-verapamil or Rh123 in the presence of digoxin (Fig. 4, A and B) showed even larger decreases in inhibitor effects between this haplotype and the common haplotype C1236T-G2677T-C3435T. Moreover, use of Rh123 in the presence of fexofenadine revealed median fluorescence of 26.9 for the wild type, 24.3 for C1236T-G2677T-C3435T, and 20.3 for C1236T-G2677T-C3435A. The median fluorescence in the presence of paclitaxel and fexofenadine was 38.2 for the wild type, 28.6 for C1236T-G2677T-C3435T, and 22.9 for C1236T-G2677T-C3435A.

The amino acid sequence of proteins is generally believed to determine protein expression, folding, and function; mutations that alter the primary structure of a protein can affect these properties. The important question addressed by this study is the role of silent mutations (i.e., those that do not affect amino acid sequence) in protein folding and function. Recent theoretical studies have suggested that codon usage is not random, and experimental studies in prokaryotes suggest that this may be so (*28*). Here we show that a silent mutation in a complex, mammalian membrane transport protein alters the substrate specificity. We hypothesize that when frequent codons are changed to rare codons in a cluster of infrequently used codons, the timing of cotranslational folding is affected (*29*) and may result in altered function. This finding may be clinically important. For example, mutations in the *MRP6* (*ABCC6*) gene cause the disease pseudoxanthoma elasticum, but missense and nonsense mutations are found in only about 60% of cases (*30*), raising the possibility that mutations that do not change coding sequence may contribute to disease by a similar mechanism.

References and Notes

1. M. M. Gottesman, T. Fojo, S. E. Bates, *Nat. Rev. Cancer* **2**, 48 (2002).
2. C. Cordon-Cardo *et al.*, *J. Histochem. Cytochem.* **38**, 1277 (1990).

3. S. Hoffmeyer *et al.*, *Proc. Natl. Acad. Sci. U.S.A.* **97**, 3473 (2000).
4. S. Drescher *et al.*, *Br. J. Clin. Pharmacol.* **53**, 526 (2002).
5. M. Goto *et al.*, *Pharmacogenetics* **12**, 451 (2002).
6. S. V. Ambudkar, C. Kimchi-Sarfaty, E. Z. Sauna, M. M. Gottesman, *Oncogene* **22**, 7468 (2003).
7. H. N. Salama, Z. Yang, T. Bui, R. J. Y. Ho, *J. Pharm. Sci.* **95**, 2293 (2006).
8. K. Tang *et al.*, *Pharmacogenetics* **12**, 437 (2002).
9. M. Horinouchi *et al.*, *Pharm. Res.* **19**, 1581 (2002).
10. L. X. Shen, J. P. Basilion, V. P. Stanton Jr., *Proc. Natl. Acad. Sci. U.S.A.* **96**, 7871 (1999).
11. L. Frittitta *et al.*, *Diabetes* **50**, 1952 (2001).
12. M. D. Perloff, L. L. von Moltke, E. Stormer, R. I. Shader, D. J. Greenblatt, *Br. J. Pharmacol.* **134**, 1601 (2001).
13. J. J. Gribar, M. Ramachandra, C. A. Hrycyna, S. Dey, S. V. Ambudkar, *J. Membr. Biol.* **173**, 203 (2000).
14. See supporting material on *Science* Online.
15. C. Kimchi-Sarfaty, J. J. Gribar, M. M. Gottesman, *Mol. Pharmacol.* **62**, 1 (2002).
16. H. T. Thi Tran *et al.*, *Mol. Genet. Metab.* **85**, 213 (2005).
17. D. Wang, A. D. Johnson, A. C. Papp, D. L. Kroetz, W. Sadee, *Pharmacogenet. Genomics* **15**, 693 (2005).
18. A. Ruth, W. D. Stein, E. Rose, I. B. Roninson, *Biochemistry* **40**, 4332 (2001).
19. T. W. Loo, D. M. Clarke, *J. Biol. Chem.* **273**, 14671 (1998).
20. I. Z. Siemion, P. J. Siemion, *Biosystems* **33**, 139 (1994).
21. S. Brunak, J. Engelbrecht, *Proteins* **25**, 237 (1996).
22. A. A. Adzhubei, I. A. Adzhubei, I. A. Krasheninnikov, S. Neidle, *FEBS Lett.* **399**, 78 (1996).
23. S. K. Gupta, S. Majumdar, T. K. Bhattacharya, T. C. Ghosh, *Biochem. Biophys. Res. Commun.* **269**, 692 (2000).
24. P. Cortazzo *et al.*, *Biochem. Biophys. Res. Commun.* **293**, 537 (2002).
25. A. A. Komar, T. Lesnik, C. Reiss, *FEBS Lett.* **462**, 387 (1999).
26. T. Xie, D. Ding, *FEBS Lett.* **434**, 93 (1998).
27. P. M. Sharp, W. H. Li, *Nucleic Acids Res.* **15**, 1281 (1987).
28. F. Supek, K. Vlahovicek, *BMC Bioinformatics* **6**, 182 (2005).
29. V. Anthony, W. R. Skach, *Curr. Protein Pept. Sci.* **3**, 485 (2002).
30. L. Bercovitch, P. Terry, *J. Am. Acad. Dermatol.* **51**, S13 (2004).

31. We thank W. Stein for fruitful discussions; R. Kincaid for a discussion that led to the idea that substitution of rare codons could affect folding of complex transmembrane proteins; G. Leiman for valuable editorial assistance; P. FitzGerald, who assisted us with codon usage rates; and S. Garfield for help with confocal images. Supported by the National Institute of General Medical Sciences Pharmacology Research Associate (PRAT) program (A.M.C.) and by the Intramural Research Program of the Center for Cancer Research, National Cancer Institute.

Supporting Online Material

www.sciencemag.org/cgi/content/full/1135308/DC1
Materials and Methods
Figs. S1 to S5
Table S1
References

19 September 2006; accepted 28 November 2006
Published online 21 December 2006;
10.1126/science.1135308
Include this information when citing this paper.

Imaging of Germinal Center Selection Events During Affinity Maturation

Christopher D. C. Allen,* Takaharu Okada,*† H. Lucy Tang,‡ Jason G. Cyster†

The germinal center (GC) is an important site for the generation and selection of B cells bearing high-affinity antibodies, yet GC cell migration and interaction dynamics have not been directly observed. Using two-photon microscopy of mouse lymph nodes, we revealed that GC B cells are highly motile and extend long cell processes. They transited between GC dark and light zones and divided in both regions, although these B cells resided for only several hours in the light zone where antigen is displayed. GC B cells formed few stable contacts with GC T cells despite frequent encounters, and T cells were seen to carry dead B cell blebs. On the basis of these observations, we propose a model in which competition for T cell help plays a more dominant role in the selection of GC B cells than previously appreciated.

Germinal centers (GC) represent critical sites within organized lymphoid tissues in which B cell responses to antigen are amplified and refined in specificity. A classical model of GC function holds that B cells in the dark zone undergo rapid rounds of proliferation and somatic hypermutation of their antibody genes, followed by exit from the cell cycle and movement to the light zone, where the B cells undergo selection based on the affinity of their surface antibody for antigen (*1*–*5*). The selection process is thought to involve competition between GC B cells for capture of antigen in the form of immune complexes displayed on the processes of follicular dendritic cells (FDCs) (*1*, *3*, *5*, *6*). However, recent experimental evidence and computer simulations have contradicted aspects of this classical model (*3*, *7*–*9*),

Howard Hughes Medical Institute and Department of Microbiology and Immunology, University of California, San Francisco, CA 94143, USA.

*These authors contributed equally to this work.
†To whom correspondence should be addressed. E-mail: Takaharu.Okada@ucsf.edu (T.O.); Jason.Cyster@ucsf.edu (J.G.C.)
‡Present address: Amgen Inc., 1120 Veterans Boulevard, South San Francisco, CA 94080, USA.

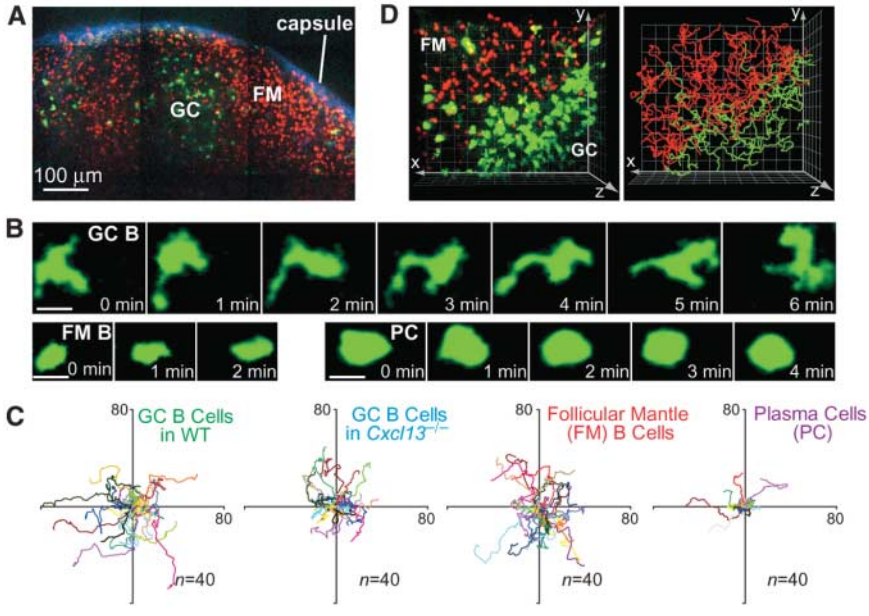

Fig. 1. Dynamics and motility of GC B cells compared with follicular mantle (FM) B cells and plasma cells (PC). (**A**) An 18-μm maximum intensity *z*-projection from two-photon microscopy image stacks of a GC and FM in an intact LN. A time-lapse recording corresponding to the center of this region is shown in movie S1. (**B**) Representative time-lapse images from two-photon microscopy showing the morphology of a GC B cell, FM B cell, and PC. The FM B cells in this experiment were naïve GFP^+ cells that were also labeled with CMTMR (*10*), and only the GFP channel is shown in the images. Scale bars, 10 μm. (**C**) Superimposed 15-min tracks of 40 randomly selected cells of each indicated type in the *xy* plane, setting the starting coordinates to the origin. Units are in micrometers. WT, wild type. Each color represents one cell's path. (**D**) (Left) Maximum-intensity projection of FM (red) and GC (green) B cells. (Right) Tracks of FM (red) and GC (green) B cells. The gridlines are separated by 20 μm.

ERRATUM

Post date 30 November 2007

Reports: "A 'silent' polymorphism in the *MDR*1 gene changes substrate specificity" by C. Kimchi-Sarfaty *et al.* (26 Jan. 2007, p. 525). Based on an inquiry from Jack Kornblatt, the authors wish to clarify that the protein sequence was obtained from a detailed mass spectrometric study performed at the Harvard Microchemistry Facility (HMF) by microcapillary reverse-phase HPLC nano-electrospray tandem mass spectrometry. HMF performed both chymotryptic and pronase digestions of the protein. In all, 82 peptides (representing 37% of the Pgp sequence by amino acid count) were identified and sequenced (see Supporting Online Material at www.sciencemag.org/cgi/content/full/318/5855/1382/DC1). Each of these sequences was identical to the sequence of haplotype P-glycoprotein. Moreover, several different peptides encoded by the synonymous SNP (3435C>T), which is the key polymorphism linked to the functional change in Pgp, were sequenced and found to be unchanged. In addition, the analysis of codon usage, Table S1 in the original Supporting Online Material (see www.sciencemag.org/cgi/data/1135308/DC1/1) contains for each codon around the three polymorphisms the frequency of this codon per 1000 codons in the human genome instead of RSCU values as stated in the text. These values were obtained from the codon usage Web site at (http://www.kazusa.or.jp/codon/cgibin/showcodon.cgi?species=Homo+sapiens+%5Bgbpri%5D). Figure 1, panels D to F, shows results in the presence of cyclosporin A (+CsA) not (+/CsA) as indicated in the body of the figure. This is correctly stated in the legend. These clarifications do not affect the conclusions of the paper.